PALEOCEANOGRAPHY, VOL. 14, NO. 2, PAGES 171-186, APRIL 1999

Diffuse spectral reflectance as a proxy for percent carbonate content in North Atlantic sediments

Joseph Ortiz

Lamont-Doherty Earth Observatory of Columbia University, Palisades, New York

Alan Mix and Sara Harris[1]

College of Oceanic and Atmospheric Sciences, Oregon State University, Corvallis

Suzanne O'Connell

Department of Earth and Environmental Sciences, Wesleyan University, Middletown, Connecticut

Abstract. Diffuse reflectance records from Feni Drift in the North Atlantic faithfully record sediment percent carbonate. A high-resolution, reflectance-based age model for these sediments derived from an orbitally tuned age model for western equatorial Atlantic, Ceara Rise sediments was generated by spectral frequency mapping. Power spectra of the Feni Drift record indicate statistically significant sub-Milankovitch cyclicity at 7.6-8.4 and 4.8-6.1 kyr. We infer that these ~8 and ~5 kyr cycles document a linkage between North and equatorial Atlantic climate given our ability to correlate these records. These climate cycles influence Atlantic basin carbonate prior to the intensification of Northern Hemisphere glaciation and thus must arise from some portion of the climate system other than the dynamics of large ice sheets. The presence of these peaks, which could be related to equatorial clipped precession, implies a possible non-linear response to Milankovitch forcing.

1. Introduction

1.1. The Search for Sub-Milankovitch Variability

While paleoceanographic study of Earth's Milankovitch-scale climate (20-100 kyr cycles) has progressed significantly in the past decades, little emphasis has been placed on the study of sub-Milankovitch-scale variability until recently. The reasons for a lack of focus on higher frequencies are largely pragmatic. Records of sufficiently high resolution and quality are only recently available. Second, much of the paleoceanographic research of the 1970's and 1980's was driven by interest in testing the veracity of the Milankovitch-Croll hypothesis, which stipulates that climate variability is driven in large part by changes in Earth's orbital geometry [*Hays et al.*, 1976; *Imbrie et al.*, 1984]. It is now fairly well accepted that variations in the Earth's orbit exert a profound influence on 20-100 kyr climate cyclicity [*Imbrie et al.*, 1992, 1993].

In contrast, sub-Milankovitch-scale variability, which is defined here as climate cycles ranging from 1 to 20 kyr, generally exhibits much less variance than its Milankovitch-band counterpart so that high-quality records with much greater temporal resolution are needed to observe it. North Atlantic Heinrich events or the Dansgaard-Oscheger (D-O) events provide examples of these processes. Likewise, no overriding central theory to explain the cause or causes of millennial or sub-Milankovitch-scale variability has been agreed upon. Climate cycles in this frequency band have been attributed to a forced harmonic response to variability in the Milankovitch bands [e.g. *Hagelberg et al.*, 1994] or to specific mechanisms arising from unforced internal oscillations in the climate system [e.g. *Ghil and LeTreut*, 1981; *Yiou et al.*, 1994]. It has been postulated, for example, that Heinrich events, which occur with a quasi-periodicity of 7-10 kyr arise from unforced oscillations due to the interactions of large ice sheets with underlying bedrock, a mechanism referred to as the "binge-purge hypothesis" [*MacAyeal*, 1993a b; *Alley and MacAyeal*, 1994].

Diffuse spectral reflectance provides a rapid, high-resolution, noninvasive tool suitable for generating high-quality records necessary for study of sub-Milankovitch climate. Here we use reflectance data collected on Ocean Drilling Program cores (Table 1) from high sedimentation rate sites in the North and equatorial Atlantic (Figure 1) to test for the presence of millennial-scale climate variability in marine sediments prior to the intensification of Northern Hemisphere glaciation. The reflectance-based proxy percent carbonate records will allow us to test the hypothesis that Heinrich-like, millennial-scale climate variability with a periodicity of 7-10 kyr was not present prior to the intensification of Northern Hemisphere glaciation. Negation of this hypothesis would suggest that the observed millennial-scale variability must arise from some portion of the climate system other than the dynamics of large ice sheets.

[1] Now at Sea Education Association (SEA), Woods Hole, Massachusetts.

Paper number 1998PA900021.
0883-8305/99/1998PA900021$12.00

Table 1. Locations, Data Types, and Sources for the Carbonate Time Series

Carbonate Method	Location	ODP Site	Latitude - Longitude	Water Depth	Age Model	Data Source
SCAT reflectance	Feni Drift	980-981	55°28.700'N 14°40.592'W	2171 m	frequency mapping to site 926	this paper
SCAT reflectance	Rockall Bank	982	57°30.760'N 15°51.251'W	1134 m	biostratigraphy and magnetostratigraphy	this paper; *Leg 162 shipboard Party* [1996b]
Coulometry	Rockall Bank	982	57°30.760'N 15°51.251'W	1134 m	n/a	*Venz et al.* [1999]
SCAT reflectance	Gardar Drift	983	60°24.210'N 23°38.440'W	1983 m	biostratigraphy and magnetostratigraphy	this paper; *Leg 162 shipboard Party* [1996c]
Coulometry	Gardar Drift	983	60°24.210'N 23°38.440'W	1983 m	n/a	*Channell et al.*, [1997]
SCAT reflectance	Bjorn Drift	984	61°25.519'N 24°04.945'W	1648 m	biostratigraphy and magnetostratigraphy	this paper; *Leg 162 shipboard Party* [1996d]
SCAT reflectance	Cearra Rise	926	03°43.141'N 42°54.498'W	3598 m	Orbitally tuned magnetic suceptibility	*Harris et al.* [1997]; *Bickert et al.* [1997]; *Tiedemann and Franz* [1997]

ODP, Ocean Drilling Program; SCAT, split-core analysis track. Average site location and depth are based on values for all holes at each site.

1.2. A North Atlantic-Equatorial Atlantic Climate Connection?

Why search for a linkage between equatorial Atlantic and North Atlantic carbonate records? Such a linkage may not be surprising. *Hughen et al.* [1996] reported a linkage on decadal to centennial timescales by correlating the fine structure of grayscale records (a proxy for sediment percent carbonate content) from the Cariaco basin in the western Atlantic with the air temperature record from the Greenland Ice Core Project (GRIP) ice core. Furthermore, they cite a number of references that document a correlation between the air-temperature variability observed in the GRIP record and a variety of North Atlantic climate proxy records [*Dansgaard et al.*, 1989; *Lehman and Keigwin*, 1992; *Koc-Karpuz and Jansen*, 1992]. On the basis of inferences from general circulation model (GCM) sensitivity studies [*Rind et al.*, 1986, *Overpeck et al.*, 1989] they conclude that decreases in North Atlantic sea surface temperature (SST) drive variations in equatorial trade wind strength, which in turn, cause variations in carbonate production within the Cariaco Basin. These carbonate shifts are recorded in the grayscale values of the underlying sediments. The correlations that *Hughen et al.* [1996] observed are striking. However, given the uncertainties in their age model on the decadal time scale and the inability to document lead-lag phase relationships between the two records, concluding that changes in North Atlantic SST are the driving factor in this relationship may be premature. Additional coupled-ocean atmosphere GCM sensitivity studies in which equatorial trade wind strength are varied and North Atlantic SST response is monitored are warranted. This would provide a means of testing the alternative hypothesis, namely that variations in equatorial wind patterns may drive shifts in North Atlantic SST.

On longer timescales, linkages between equatorial winds and North Atlantic climate have also been reported. *McIntyre and Molfino* [1996] observed variability in the depth of the equatorial nutricline with a periodicity of 7.6 kyr which is presumably driven by changes in equatorial winds. *McIntyre and Molfino* [1996] speculate that the origin of this periodicity arises from a harmonic interaction of precession and eccentricity forcing during times of weak eccentricity forcing of anomalously short period. Their evidence for these climatic changes are shifts in the abundance of the nutricline dwelling coccolithophorid *Florisphaera profunda.* The relative importance of this species within the coccolithophorid community increases when equatorial winds relax, which deepens the equatorial nutricline and vice versa [*Molfino and McIntyre*, 1990]. *McIntyre and Molfino* [1996] document a correspondence between the timing of peaks in the *F. profunda* record from RC24-08 and the Heinrich events as recorded in the ice-rafted debris (IRD) record from V23-81 [*Bond and Lotti*, 1995]. In contrast to *Hughen et al.* [1996], *McIntyre and Molfino* [1996] infer that the equatorial heat engine, through its influence on low-latitude wind strength, drives variations in high-latitude climate. Use of reflectance data generated on two separate Ocean Drilling Program (ODP) legs will allow us to explore the potential linkages between the equatorial Atlantic and the North Atlantic on a variety of timescales and in sediments much older than can be recovered with standard piston coring methods.

2. Methods

Sediment diffuse reflectance was measured at sea during ODP Leg 162 using the Oregon State University (OSU), split-core analysis track (SCAT). The Leg 162 configuration of the SCAT (Fig-

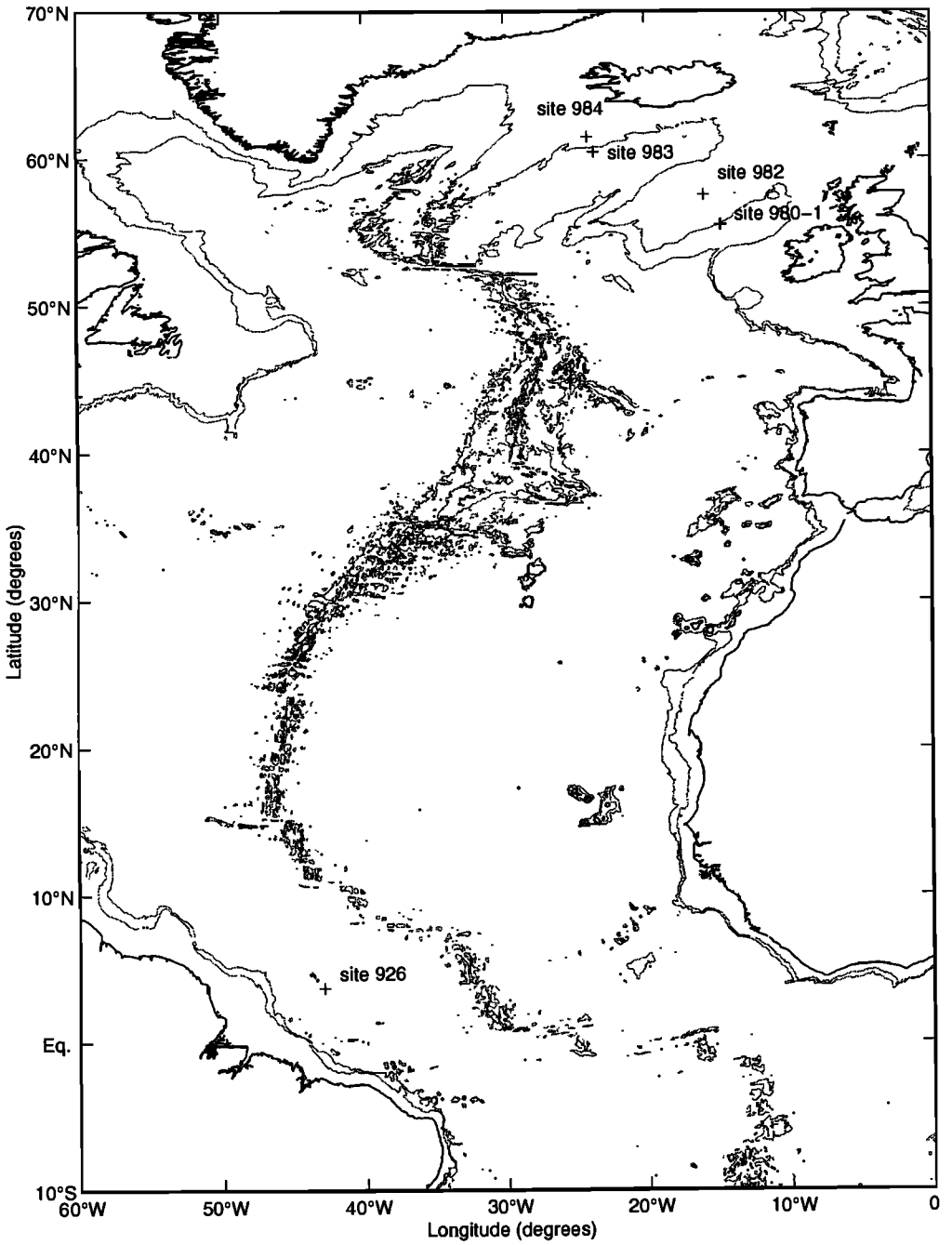

Figure 1. The locations of Ocean Drilling Program (ODP) sites 980-984 in the North Atlantic and site 926 on the Ceara Rise in the western equatorial Atlantic.

ure 2) was first used during postcruise operations on ODP Leg 154 [*Harris et al.*, 1997]. Reflectance measurements with this version of the instrument have a signal-to-noise ratio that is an order of magnitude greater than the prototype instrument deployed during ODP Leg 138 [*Harris et al.*, 1997; Mix *et al.*, 1992]. *Ortiz et al.*, [1999] provide a more detailed description of the instrument's operation. During ODP coring operations, consecutive 10 m long sediment cores are raised from the deep sea and cut on deck into six or seven whole-round sections up to 1.5 m in length. The sections are allowed to reach ambient temperature, then are split in half lengthwise for immediate description, analysis, and sampling in the ship's corelab. SCAT reflectance measurements were conducted by the shipboard sedimentologists on the lightly scraped archive half of each wet sediment section immediately after splitting and during the core description process. The split core sections were not covered with Glad-wrap™ during measurement [e.g., *Leg 154 Shipboard Scientific Party*, 1995; *Balsam et al.*, 1997]. While this precaution is necessary to protect the integrating

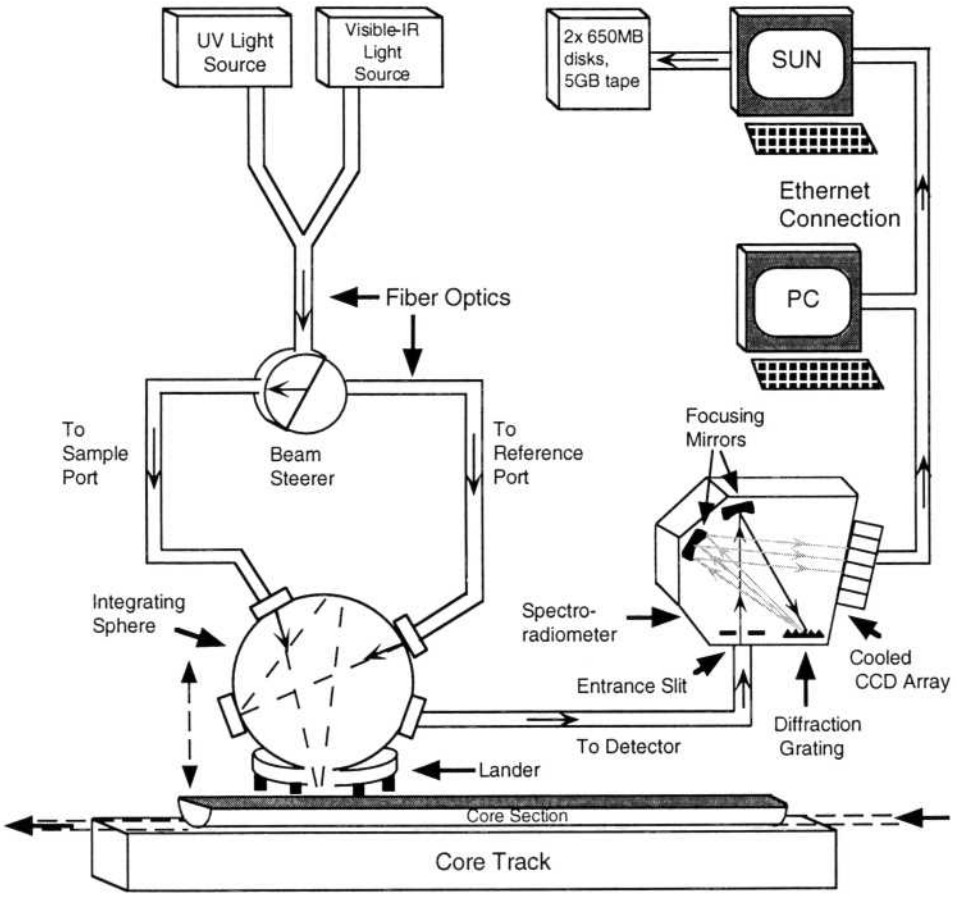

Figure 2. A schematic illustration of the major components of the Oregon State University split-core analysis track (OSU SCAT). Reprinted from *Ortiz et al.* [1999] with permission of the Ocean Drilling Program.

sphere of the hand-held Minolta CM-2002 spectrophotometer because of its measurement geometry, it is not needed with the automated SCAT.

The SCAT measurements were generally taken at 8 cm intervals, although higher-resolution measurements (4 cm resolution) were taken when time permitted. To ensure that composite reflectance splices could be generated, cores from additional holes drilled at each site were selected for analysis on the basis of concurrent gamma ray attenuation porosity estimator (GRAPE) or magnetic susceptibility data. Because of time constraints, the sediments from 0 to ~90 meters composite depth (MCD) at site 981 on the Feni Drift were not analyzed because this sediment sequence represents a lower sedimentation rate repeat of the shallow sediments at site 980, another coring site drilled on the Feni Drift [*Leg 162 Shipboard Scientific Party*, 1996a]. The reflectance records from the two Feni Drift sites (site 980 and 981) can be easily spliced in the age domain to yield a composite record.

3. Results and Discussion

3.1. Reflectance-Based Proxy Percent Carbonate

Postcruise data processing of the SCAT data set consisted of quality control to assure that there were no measurement offsets and averaging the 1024-channel data into a 70-channel (10 nm resolution) percent reflectance data set. The 10 nm resolution reflectance data were used to calculate a center-weighted, first-derivative spectra for each reflectance sample consisting of 68 first-derivative channels. The first-derivative of the reflectance spectra ($\partial R/\partial\lambda$) defines the "spectral shape" of the sample. It is useful for assessment of trace minerals such as hematite and goethite [*Balsam and Deaton*, 1991; *Deaton and Balsam*, 1991]. We employed center-weighted first-derivatives, the average of $\partial R/\partial\lambda$ for the reflectance bands above and below the wavelength band of interest because they are numerically more stable [*Press et al.*, 1992] than first-difference derivatives. The processed 10 nm reflectance and first-derivative data are archived on CD-ROM by *Ortiz et al.*, [1999].

Using the 10 nm reflectance and first-derivative data, we generated a stepwise, multiple linear regression to estimate proxy percent carbonate from paired shipboard percent carbonate [*Leg 162 Shipboard Scientific Party*, 1996a,b,c,d] and reflectance measurements. Following *Mix et al.* [1995] and *Harris et al.* [1997], we also use the square of the 10 nm reflectance bands as potential input variables for the regression. While empirical, this approach has been used successfully by *Mix et al.* [1995] and *Harris et al.* [1997] because it allows the reflectance equation to incorporate a curvilinear response to variations in percent carbonate. Shipboard percent carbonate measurements were matched to the closest reflectance measurements within 5 cm. Percent carbonate samples

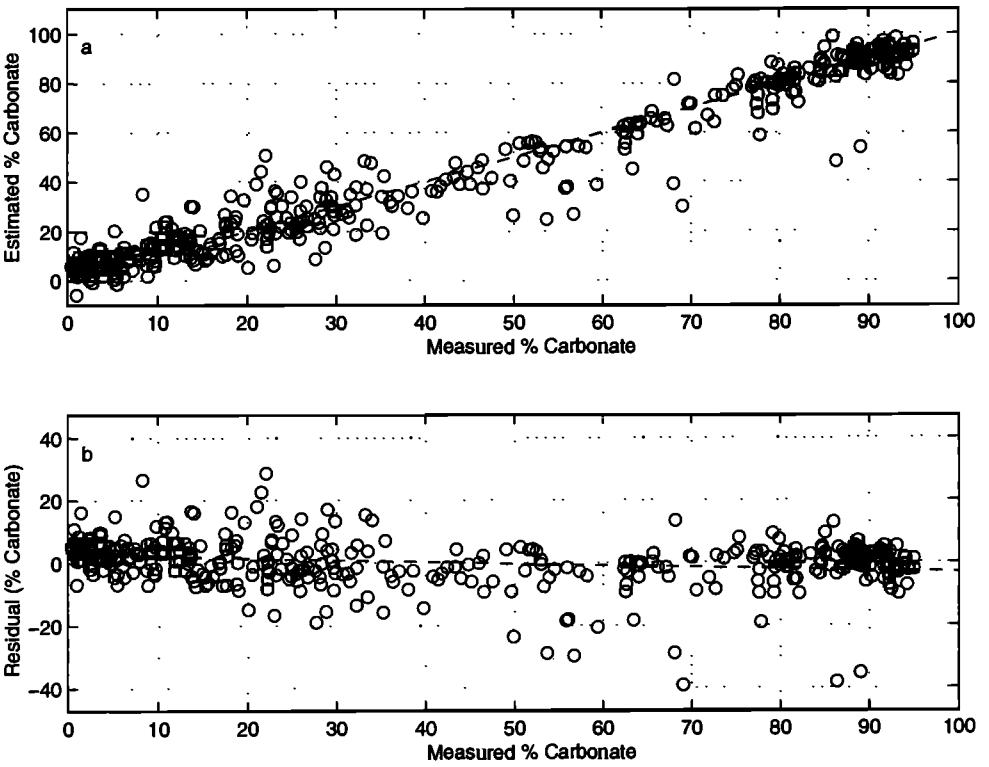

Figure 3. (a) Percent carbonate measured by coulometry versus percent carbonate estimated by diffuse spectral reflectance for ODP sites in the North Atlantic. (b) Residual errors in reflectance-based carbonate estimates as a function of carbonate measured by coulometry.

with reflectance measurements that were farther than 5 cm were not included in the analysis. The multiple regression equation is based on 384 reflectance-percent carbonate pairs from the North Atlantic sites drilled during Leg 162 (sites 980-984). It has the form

$$\text{proxy\% } CaCO_3 = -3.50R_{465} + 6.65R_{525} - 2.60R_{815}$$

$$+ 2.91R_{925} + 0.03(R_{465})^2 - 0.06(R_{555})^2 - 9.23$$

where R_λ represents the 10 nm reflectance band centered on wavelength λ. None of the first-derivative terms were significant in the final stepwise multiple linear regression. Several of the terms in the regression have wavelengths toward the blue end of the visible spectrum (465, 525, and 555 nm) where carbonate exhibits its maximum diffuse reflectance [Mix *et al.*, 1995] or in the near infrared (815 and 925 nm), indicating the potential importance of clay minerals or oxides. The regression terms are thus physically meaningful as these sediments represent in large part a mixture between carbonate and lithogenic material of both marine and continental origin. The unforced regression equation is statistically significant ($p<<0.001$) and accounts for 94.2% of the observed percent carbonate variance with a root mean square error (RMSE) of 8.0%. Comparison of coulometrically measured percent carbonate with the reflectance-based carbonate estimates demonstrates little statistical bias (Figure 3). Outliers that are evident in the measured vs. estimated (Figure 3a) and residual plots (Figure 3b) likely result from depth mismatches between reflectance and percent carbonate measurements at site 980, where percent carbonate variations with depth are abrupt. The reflectance-based carbonate estimates are given in Appendix A1.[1]

The character of the resulting carbonate records varies dramatically from southeast to northwest when plotted using a preliminary age model based on biostratigraphic and magnetostratigraphic datums determined during the research cruise (Figure 4). Measurements from Feni Drift in the Rockall Trough (sites 980 and 981) and on the Rockall Bank (site 982) exhibit a typical North Atlantic carbonate pattern, similar to that observed at site 607 or other ODP sites further to the south [*Ruddiman and Raymo*, 1988; *Raymo et al.*, 1989]. In contrast, carbonate measurements from the Gardar (site 983) and Bjorn (site 984) Drifts along the Reykjanes Ridge exhibit carbonate variations that while similar to each other, are radically different from the Rockall sites due to carbonate dilution by fine grained terrigenous sediment.

We verify the calibration of the proxy percent carbonate equation by comparison to two extensive carbonate data sets (Figure 5) totaling 1900 observations from Rockall Bank [*Venz et al.*, 1999] and Gardar Drift [*Channell et al.*, 1997] sediments. Data from these two sites span the full range of percent carbonate and percent reflectance variability observed during Leg 162. Quantita-

[1] Appendix A1 is available electronically at World Data Center-A for Paleoclimatology, NOAA/NGDL, 325 Broadway, Boulder, Colorado (e-mail: paleo@mail.ngdl.noaa.gov; URL: http://www.ngdl.noaa.gov/paleo).

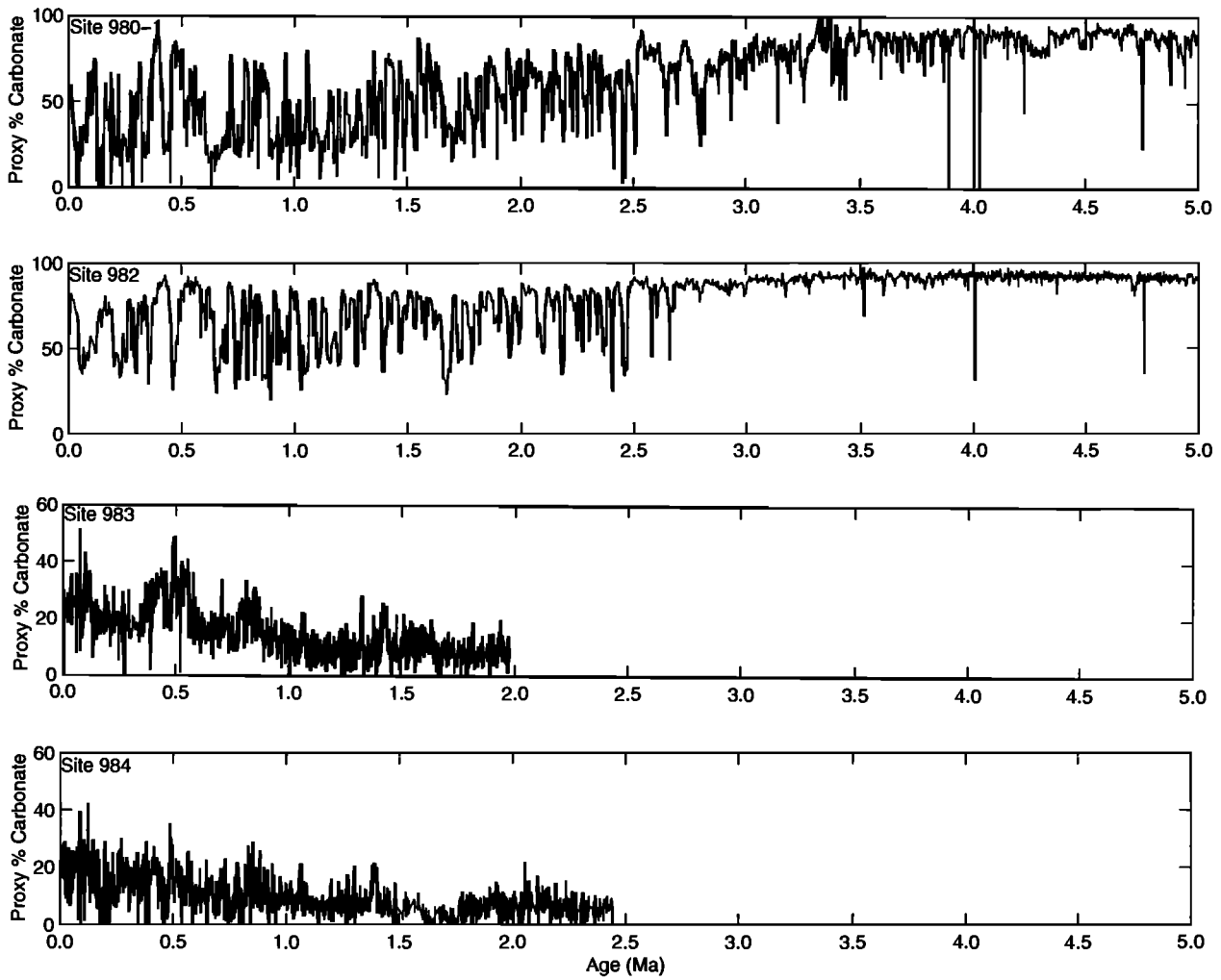

Figure 4. North Atlantic carbonate estimates derived from percent reflectance using the transfer function described in the text. Data are plotted as a function of age using a preliminary age model based on biostratigraphy and magnetostratigraphy.

tive comparison of these percent carbonate data with the proxy percent carbonate predictions for the same depth interval reveal an RMSE of 8.0 and 5.6% at sites 982 and 983, respectively. While the RMSE at the Gardar Drift is smaller than for the Rockall Bank record, the proxy percent carbonate regression performs better in the brighter sediments at the Rockall Bank (Figure 5). The reason for this is simple: when percent carbonate content becomes low, it exerts less influence on sediment brightness. While fine-scale percent carbonate features at the Gardar Drift are recorded by the proxy percent carbonate record, there is a tendency to overestimate carbonate content when percent carbonate content drops below ~20%. In the remainder of this paper we focus our attention on time series analysis of the proxy percent carbonate record from the brighter sediments at Feni Drift where sedimentation rates are high (~10 cm kyr^{-1}), and a continuous record back to 4.5 Ma is available.

3.2. A High Resolution Reflectance-Based Timescale

A prerequisite to time series analysis of the reflectance-derived proxy carbonate record at Feni Drift is a reliable, high-resolution age model. Careful inspection of Figure 4 indicates apparent temporal "offsets" between clearly synchronous carbonate events at sites 980-1 and 982. This is perhaps most clearly illustrated in the time interval between 2.5 and 3 Ma. The most likely cause for these offsets are changes in sedimentation rate between the two sites, pointing out the need for a high-resolution age model. Developing such a model could be accomplished by generating an oxygen isotope stratigraphy for sediments from Feni Drift or by applying an existing age model from another site to the proxy percent carbonate record at Feni Drift. Because the generation of oxygen isotope chronologies for the Leg 162 sediments entails ongoing research at several isotope laboratories, a composite oxygen

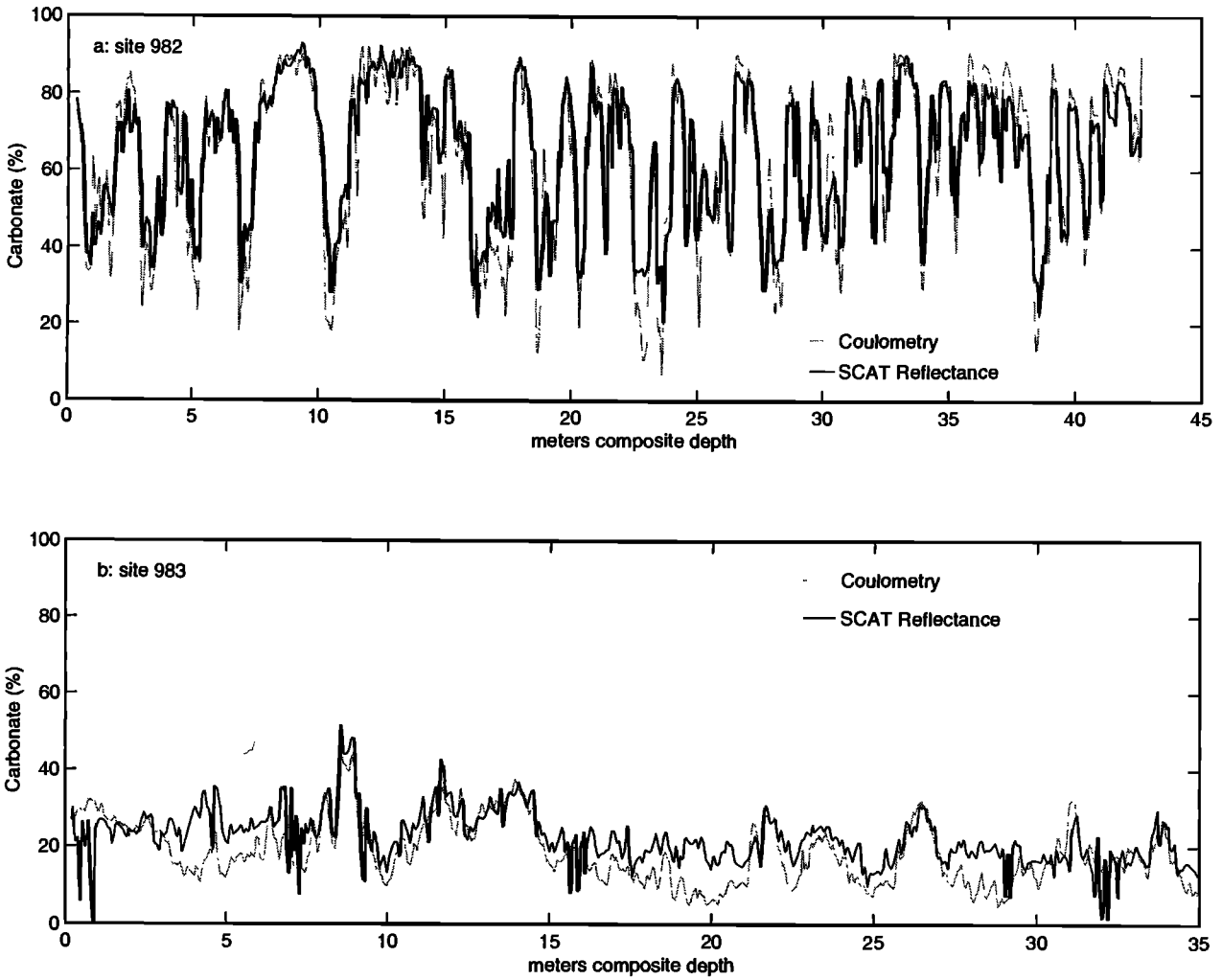

Figure 5. Validation of the reflectance-derived carbonate transfer function using coulometric carbonate data from (a) the Rockall Bank (site 982) and (b) the Gardar Drift (site 983). The 5 cm resolution coulometric carbonate measurements were smoothed with a two point running mean to approximate the 4-8 cm resolution of the reflectance measurements. Coulometric carbonate data from *Venz et al.* [1999] (site 982 on the Rockall Bank) and *Channell et al.* [1997] (site 983 on the Gardar Drift) are independent of the data used to construct the transfer function presented in the text.

isotope timescale for Feni Drift is not yet available for our use. Accordingly, we have adopted the latter strategy.

Our approach is to use the inverse, frequency-mapping method of *Martinson et al.* [1987] to determine the optimal correlation between the reflectance-based proxy percent carbonate record from site 926 on the Ceara Rise (ODP Leg 154) and the reflectance-based proxy percent carbonate record from Feni Drift generated as part of this study. A similar mapping strategy was employed by *Harris et al.* [1997] to correlate the reflectance records from the ODP Leg 154 sites. This methodology allows us to map the proxy percent carbonate record from Feni Drift onto the orbitally tuned timescale for site 926 on the Ceara Rise. The basic assumption embedded in this procedure is that climatically driven, carbonate dilution or dissolution events in the North Atlantic at Feni Drift and western equatorial Atlantic on the Ceara Rise vary in phase.

We selected the reflectance record from site 926 as a target curve for several reasons. First, the orbitally tuned magnetic susceptibility age model for the Leg 154 Ceara Rise sediments was derived on sediments from site 926. Orbital tuning of the magnetic susceptibility records at the Ceara Rise sites is a viable strategy because of the continuous nature of the magnetic susceptibility records and the fact that variations in magnetic susceptibility are driven by changes in the bulk properties of the sediments, namely the dilution of carbonate by terrigenous input. It is reasonable to infer that this process will have an orbital response. The timescale for site 926 was devised by *Bickert et al.*, [1997] and *Tiedemann and Franz* [1997], who orbitally tuned the Ceara Rise magnetic susceptibility record to the La93(1,1) orbital solution of *Lasker et al.*, [1993]. The La93(1,1) orbital solution is a generalized extension of the La90(0,1) orbital solution [*Lasker et al.*, 1990]. It differs from the La90(0,1) by accounting for lunar tidal effects on

Earth's orbit in addition to "dynamical variability" in the eccentricity of the Earth's orbit. Second, the reflectance records for site 926 and the other sites on the Ceara Rise were generated by the OSU SCAT so that the data are directly comparable to our data from Feni Drift. Finally, as both site 926 on the Ceara Rise (3598 m) and site 980 on the Feni Drift (~2171 m) are bathed by North Atlantic Deep Water (NADW) during interglacial periods, we expect that they should exhibit similarities in their percent carbonate records.

The intercorrelation of these records could be accomplished in either the wave (time) domain or in the frequency domain. Mapping in the wave domain consists of establishing discrete "tie points" between a reference or target curve and the record being operated on. In contrast, the inverse method of *Martinson et al.* [1987] operates largely in the frequency domain, although an initial age model (tie points) must be supplied. To test the sensitivity of the orbital solution to this initial condition, we ran simulations in which we added noise in the form of "erroneous" age-depth pairs. In all cases this spurious information was rejected during the iterative solution, resulting in a relatively stable result. Working in the frequency domain has the advantage of determining the offsets between the two records based on comparison of a multivariate statistical measure of the two time series: their Fourier transform, rather than a univariate statistical measure, the correlation coefficient. The frequency-mapping method generally leads to more continuous sedimentation rates and removes much of the arbitrariness inherent in correlating two time series by the addition of individual tie points. The analogous concept to the tie point in the inverse mapping method is the number of Fourier coefficients needed to map (or relate) the operating signal onto the reference signal.

To map the Ceara Rise age model [*Bickert et al.*, 1997; *Tiedemann and Franz* 1997] onto the Feni Drift proxy carbonate record, we placed the data from the Feni Drift cores onto preliminary age models based on biostratigraphic and magnetostratigraphic datums [*Leg 162 Shipboard Scientific Party*, 1996a]. We then re-

Table 2. Statistics for Frequency Mapping the Ceara Rise Age Model Onto Feni Drift Sediments

Shipboard Age Model, Ma	Site 926 Age Model, Ma	Number of Coefficients	Squared Correlation, r^2
	Site 980		
0.0007-0.9905	0.0000-1.0000	40	0.704
0.9905-1.6627	1.0000-1.6620	40	0.847
	Site 981		
1.6612-2.6490	1.6620-2.6260	40	0.604
2.6490-3.7117	2.6260-3.7170	48	0.657
3.7117-4.6615	3.7170-4.6590	40	0.470
	Site 981 Mapped to Site 980 Where Reflectance Signals Overlap		
1.4961-1.6612	1.5148-1.6620	16	0.934

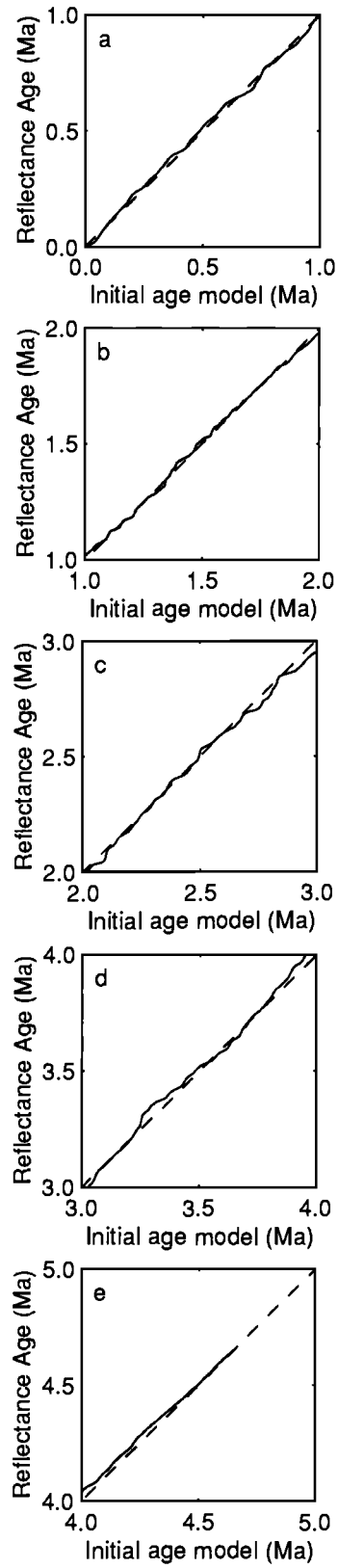

Figure 6. Feni Drift age-age mapping function for (a) 0 - 1, (b) 1 - 2, (c) 2 - 3, (d) 3 - 4, and (e) 4 - 5 Ma time intervals. The mapping function is derived by inverse correlation of the reflectance-derived carbonate records from the sites on Feni Drift and the Ceara Rise as explained in the text.

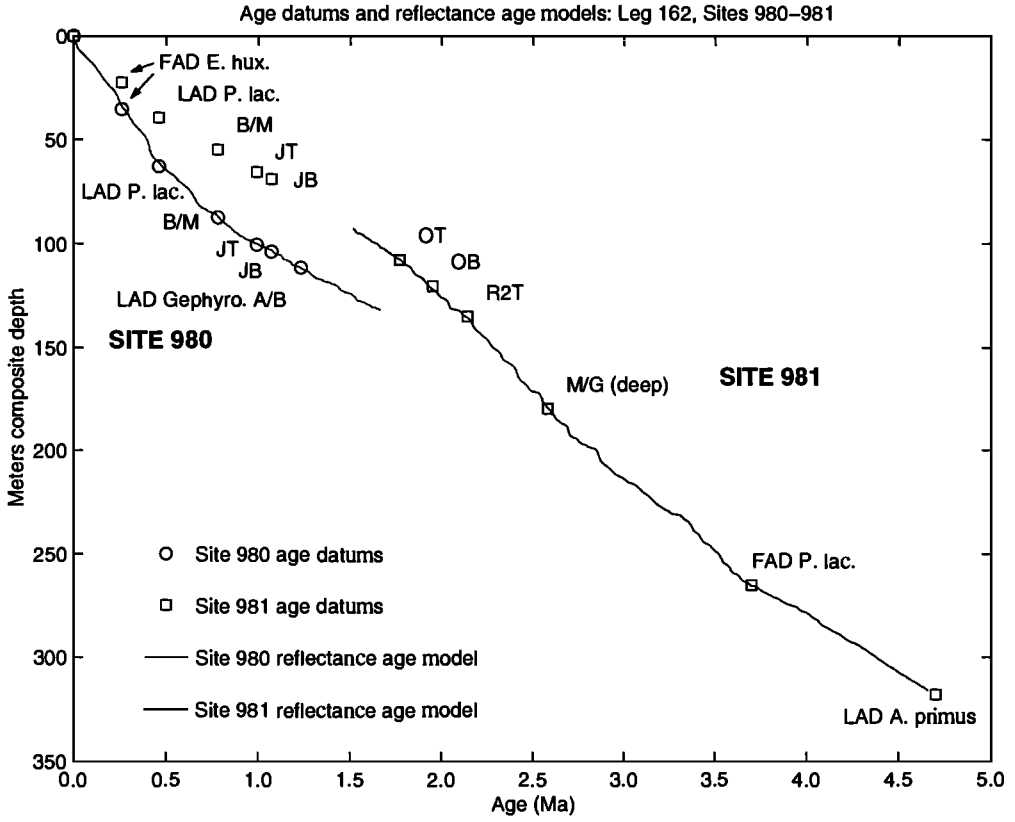

Figure 7. Depth-age plot for Feni Drift records from site 980 and site 981, ODP Leg 162. Open circles and stars refer to biostratigraphic and paleomagnetic datums determined for sediments from sites 980 and 981, respectively [*Leg 162 Shipboard Scientific Party*, 1996a]. Solid lines represent the high-resolution age models developed by frequency mapping the reflectance-based carbonate record from sites 980 and 981 onto the reflectance-based carbonate record from Ceara Rise. For biostratigraphic events, FAD refers to first-appearance depth, while LAD refers to last-appearance depth. Abbreviations for marker species are E. hux., *Emiliania huxleyi*; P. lac, *P. lacunosa*; Gephyro A/B, *Gephyrocapsa spp.* A/B, and A. primus, *A. primus*. Magnetostratigraphic events are B/M, Brunhes/Matuyama boundary; JT, top of Jaramillo; JB, bottom of Jaramillo; OT, top of Olduvai; OB, bottom of Olduvai; R2T, top of Reunion 2; and M/G (Deep), Matayama/Gauss boundary (deeper pick).

sampled all three records at 1 kyr, which is greater than or equal to the nominal sample spacing of the Feni Drift records but which oversamples the Ceara Rise record by a factor of ~2. This compromise allowed us to retain the additional information within the Feni Drift record, rather than starting with a degraded signal for correlation. The record was then divided into six subsections that were independently mapped (Table 2). This step was necessary because of limitations in available computer resources, but also allows us to evaluate the fit between the two records as a function of time. The final results were independent of the way in which the record was subdivided and imply only minor modifications to the shipboard-derived ages at Feni Drift, especially from 0 to 3 Ma (Figure 6). We qualitatively evaluate the reliability of the mapping operation on the basis of the depth-age plot for Feni Drift. The resulting high-resolution age model is consistent with the observed shipboard biostratigraphic and paleomagnetic age datums [*Leg 162 Shipboard Scientific Party*, 1996a] for these two sites (Figure 7). This gives us confidence in the quality of the high resolution reflectance based age model. In all but the oldest section of the record (3.7-4.7 Ma) the squared correlation coefficient (r^2, a measure of common variance) exceeds 0.6 with values as high as 0.85, indicating the high quality of the fit between the two records (Table 2). Lower correlation between 2.7 and 3.3 Ma may result from a mismatch in age between the two records. Despite this caveat the correlation between the two records is striking.

This frequency-mapped age model for Feni Drift was developed without the direct use of oxygen isotope data, although the method depends on an assumption of constant magnetic susceptibility phasing relative to orbital forcing as part of the orbital-tuning process [*Bickert et al.*, 1997; *Tiedemann and Franz*, 1997]. The powerful approach described here has the advantages of being nondestructive to core material at all steps, inexpensive, and less time consuming than generating an oxygen isotope stratigraphy. We conservatively estimate that the age model generated in this way has uncertainties of ~4 kyr given the sampling resolution of 1-2 kyr for the proxy percent carbonate records at Feni Drift and Ceara Rise, respectively, provided that changes in carbonate are the primary features of variance. The disadvantage of this approach is that it precludes us from assessing phase relationships of the Feni Drift proxy percent carbonate record relative to the

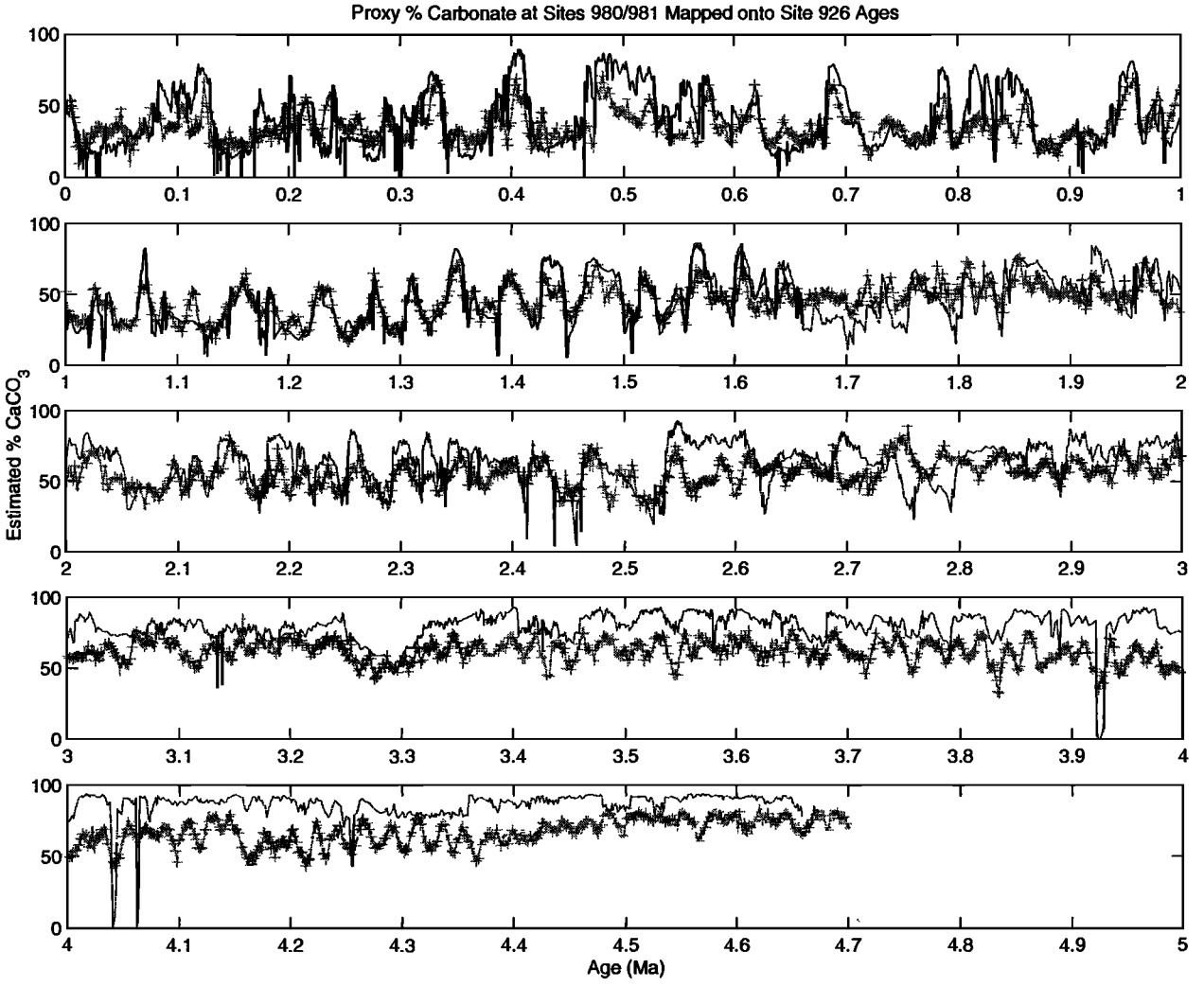

Figure 8. Reflectance-derived carbonate records for site 926 on the Ceara Rise and sites 980 and 981 on the Feni Drift plotted on the Ceara Rise age model using the age-age mapping function derived as part of this study.

Ceara Rise proxy percent carbonate mapping target. This shortcoming can be overcome by using oxygen isotopes for age constraints when that data become available.

3.3. Cyclicity of the Feni Drift Proxy Percent Carbonate Record

Spectral analysis provides a means of quantifying the periodicities in the Feni Drift proxy percent carbonate record and studying how variance in the climate system changes with time. An inherent assumption of the method is that the time series studied is stationary. However, prior studies of the climate system demonstrate shifts in the dominant frequency of climate variability at ~2.5 (or 2.75) and at 0.95 Ma. The causes of these transitions are not well understood. To accommodate these changes in the proxy percent carbonate record, we divided the proxy percent carbonate time series into three subrecords for separate spectral analysis: 0-0.95, 0.95-2.4, and 2.8-4.5 Ma. Because the non-stationarity in the proxy carbonate data appears greater than in the oxygen isotope data, we decided against the use of evolutive spectral methods.

The transition at ~2.5 Ma is believed to record the intensification of Northern Hemisphere glaciation in response to the growth of larger ice sheets. This transition is clearly evident in long benthic $\delta^{18}O$ records from the Atlantic [e.g. *Clemens and Tiedemann*, 1997]. Records of other climate proxies such as percent carbonate or from other ocean basins sometimes demonstrate an earlier transition, closer to 2.75 Ma [e.g., *Jansen and Sjoholm*, 1991; *Haug et al.*, 1995; *Maslin et al.*, 1995]. The proxy carbonate record from Feni Drift exhibits its first sustained carbonate decreases at ~2.8 Ma as well as a near step-function decrease in carbonate content at ~2.55 Ma (Figure 8). This suggests the possibility that the observed differences in timing of this event may arise from comparison of multiple events rather than a single time-transgressive process. To deal with this nonstationarity in the record, we will exclude the portion of the records from 2.4 to 2.8 Ma from our spectral analysis. The transition at 0.95 Ma (sometimes referred to as the "Mid-Pleistocene Revolution") denotes the transition from a climate regime dominated by the 41 kyr obliquity-related cycle to the 100 kyr cycle of the late Pleistocene. Sep-

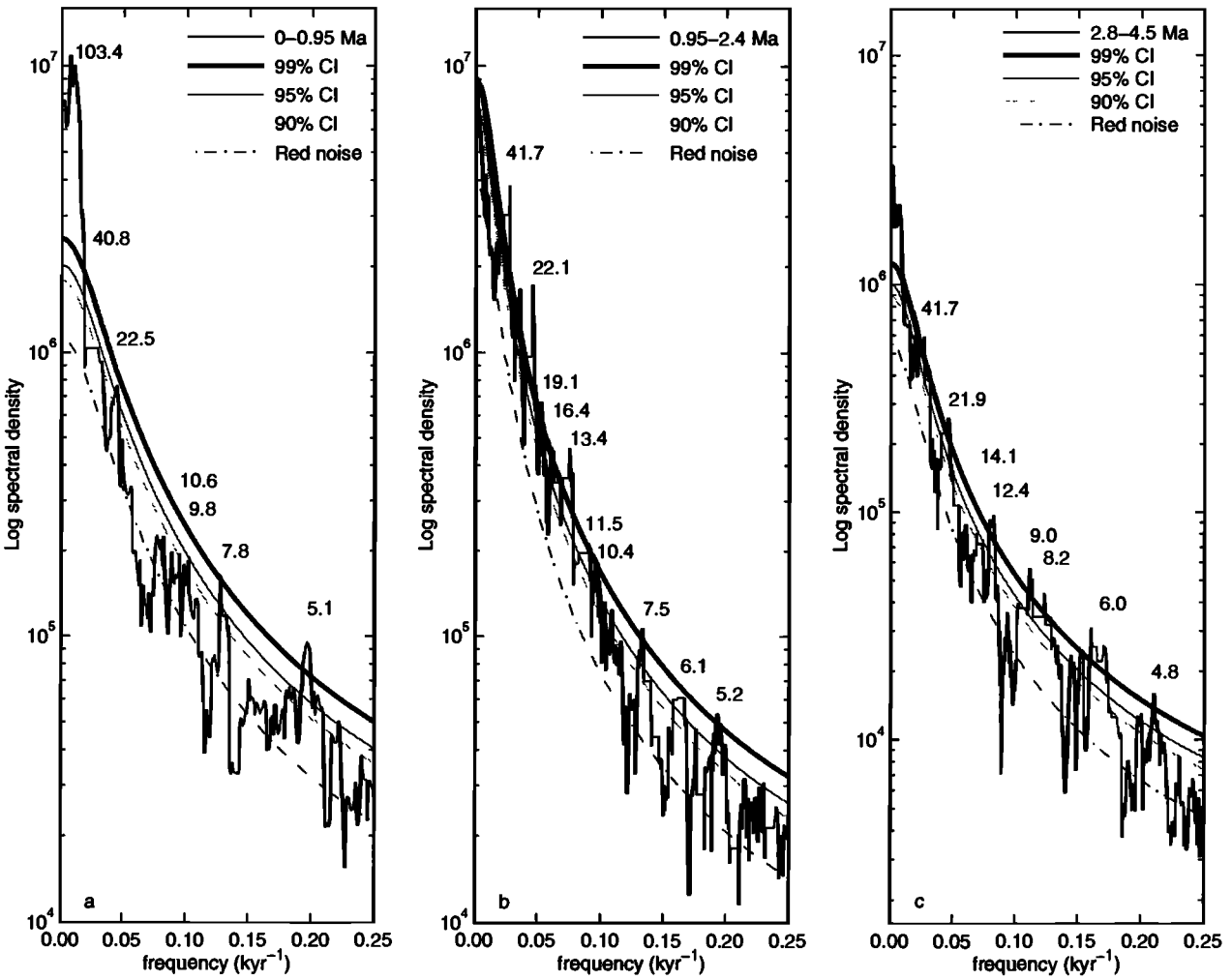

Figure 9. Multitaper power spectra for proxy percent carbonate at Feni Drift for time interval from (a) 0 to 0.95, (b) 0.95 to 2.4, and (c) 2.8 to 4.5 Ma. All spectra are calculated with a time-bandwidth resolution of four and seven tapers. Significance levels at 90%, 95%, and 99% are derived from confidence intervals relative to a robust, median, red noise background [*Mann and Lees*, 1996]. Significant spectral peaks are labeled by period in kyr.

arating the record at 0.95 Ma appears sufficient to deal with this transition in the Feni Drift carbonate record.

Spectral analysis was conducted using the Thompson multitaper method [*Thompson*, 1982]. Given the uncertainty of the age model, we present the frequency spectra from 0 to 0.25 kyr^{-1}, rather than plotting to the Nyquest frequency (0.5 kyr^{-1}). High-resolution spectra were calculated using seven tapers and a time-bandwidth resolution of four (Figure 9). These parameters were used to provide better resolution of the high-frequency (sub-Milankovitch) variability in the record. A trade-off of this approach is that we expect some smearing of variance in the primary Milankovitch bands. Significance testing of spectral peaks (Figure 9 and Table 3) was accomplished by comparison of the power spectra of the data with a robust, median, red noise background based on a first-order Markov model [*Mann and Lees*, 1996]. This model has the same white noise variance and first-order autocovariance as the data for each time period analyzed. Several interesting characteristics are seen in the data.

Significant spectral peaks in the Milankovitch band were observed with nominal periods ranging from 100 to 19 kyr (Figure 9 and Table 3). As has been previously observed [*Ruddiman and McIntyre*, 1984], the 100 kyr cycle is dominant from 0 to 0.95 Ma, while 41 kyr (obliquity-related variability) is dominant in the older sections of this high-latitude record. The stochastic variability in the climate system, characterized by the median, red noise background, and measured at the same frequencies as the spectral peaks, increases with time (Table 3). Sub-Milankovitch variability with nominal periodicities ranging from 16 to 5 kyr was also observed (Figure 9 and Table 3). The longer of the sub-Milankovitch periodicities, those ranging from ~16 to ~11 kyr, were not present as significant features throughout the record (Figure 9 and Table 3). This was not the case for the high-frequency cycles at ~10, ~8, and ~5 kyr. Because of the increase in background stochastic variance at all frequencies, the variance in the sub-Milankovitch peaks tends to increase with time. However, the variance in these bands relative to the red noise background does not indicate

Table 3. Power Spectral Characteristics of the Feni Drift Proxy Percent Carbonate Record

	0 - 0.95 Ma Spectrum				0.95 - 2.4 Ma Spectrum				2.8 - 4.5 Ma Spectrum			
Nominal Period	Observed Period and Significance Level, kyr (%)	Spectral Density, log units	Red Noise Density, log units	Relative Spectral Density	Observed Period and Significance Level, kyr (%)	Spectral Density, log units	Red Noise Density, log units	Relative Spectral Density	Observed Period and Significance Level, kyr (%)	Spectral Density, log units	Red Noise Density, log units	Relative Spectral Density
					Milankovitch Bands							
100 kyr	103.4 (>99%)	9.9×10^6	1.0×10^6	9.9x								
41 kyr	40.8 (>90%)	1.0×10^6	7.0×10^5	1.4x	41.7 (>99%)	3.0×10^6	9.7×10^5	3.1x	41.7 (>99%)	5.5×10^5	2.4×10^5	2.3x
23 kyr	22.5 (>95%)	7.6×10^5	3.8×10^5	2.0x	22.1 (>99%)	1.6×10^6	3.3×10^5	4.8x	21.9 (>99%)	2.6×10^5	9.5×10^4	2.7x
19 kyr					19.1 (>99%)	6.7×10^5	2.5×10^5	2.7x				
					Sub-Milankovitch Bands							
16 kyr					16.4 (>99%)	4.3×10^5	1.9×10^5	2.3x				
14 kyr									14.1 (>90%)	7.2×10^4	4.4×10^4	1.6x
13 kyr					13.4 (>99%)	4.6×10^5	1.3×10^5	3.5x	12.4 (>90%)	8.6×10^4	3.5×10^4	2.5x
11 kyr	10.6 (>90%)	1.9×10^5	1.2×10^5	1.6x	11.5 (>95%)	1.9×10^5	9.7×10^4	2.0x				
10 kyr	9.8 (>90%)	1.8×10^5	1.0×10^5	1.8x	10.4 (>95%)	1.6×10^5	8.0×10^4	2.0x	9.0 (>99%)	5.3×10^4	1.9×10^4	2.8x
8 kyr	7.8 (>99)	1.6×10^5	7.0×10^4	2.3x	7.5 (>99%)	1.0×10^5	4.3×10^4	2.3x	8.2 (>99%)	4.3×10^4	1.6×10^4	2.7x
6 kyr					6.1 (>99%)	6.1×10^4	3.0×10^4	2.0x	6.0 (>99%)	2.2×10^4	9.3×10^3	2.4x
5 kyr	5.1 (>99%)	9.5×10^4	3.3×10^4	2.9x	5.2 (>99%)	5.3×10^4	2.2×10^4	2.4x	4.8 (>99%)	1.6×10^4	6.1×10^3	2.6x

No value indicates no significant peak.

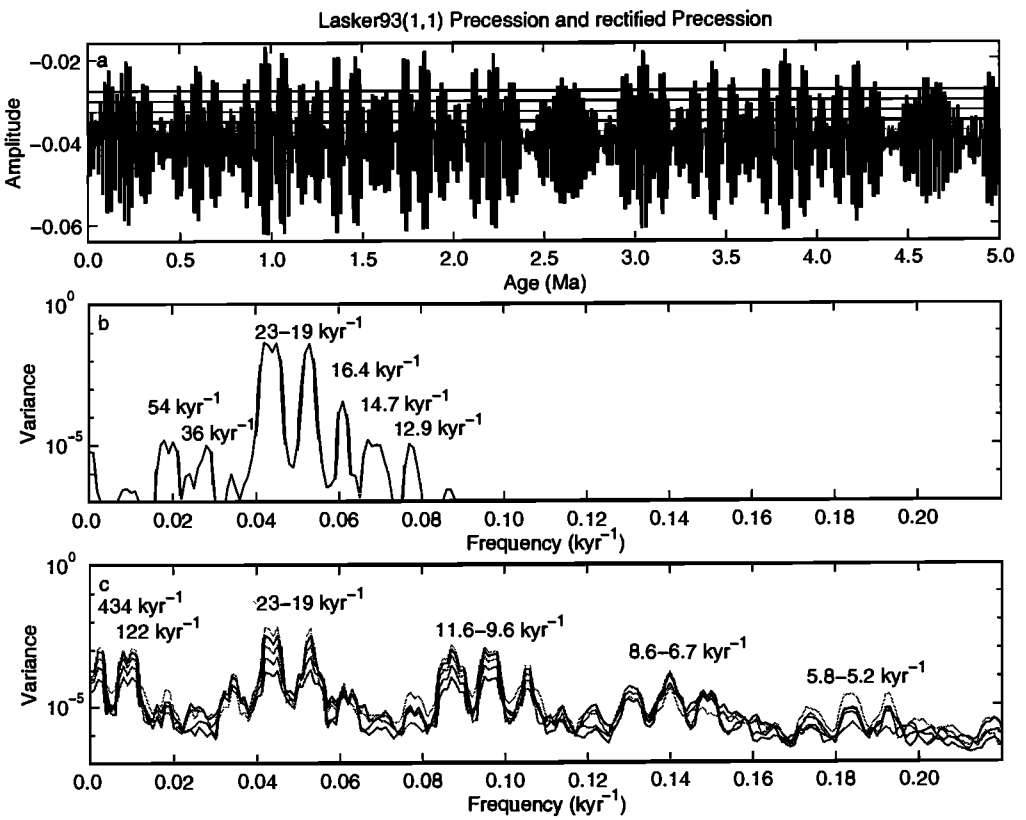

Figure 10. (a) Precession record for 0 - 5 Ma from *Lasker et al.* [1993]. Horizontal lines represent rectification thresholds used for clipping the precession curve. (b) Power spectra of the precession record plotted in Figure 10a, (c) Power spectra for precession record rectified at the levels indicated in Figure 10a.

a clear trend of increasing or decreasing sub-Milankovitch variability. Thus, while their variance increases with time, it does not appear to do so at a rate that is greater than the stochastic red noise background. This suggests that variance within the sub-Milankovitch frequencies may be relatively insensitive to changes induced by the intensification of Northern Hemisphere glaciation.

Spectral peaks at periods similar to the longer of the observed sub-Milankovitch cycles (~16, ~14, and ~13 kyr) are present in the precession band forcing, although they are significantly less energetic than the primary doublets at 23 and 19 kyr (Figure 10b and Table 3). While the peak at 16 kyr in the data spectrum (Figure 9c) is most likely independent of the peaks at 13 and 14 kyr, it is unclear if the latter represent independent concentrations of variance or a single peak at 13 or 14 kyr split by potential age model errors. Power near 13-14 kyr could arise as a harmonic of the primary orbital frequencies in a number of ways [e.g., *Yiou et al.*, 1994]. For example, it could be related to (1) an interaction of the 19 kyr precession doublet and the 41 kyr obliquity cycle (1/19+1/41 = 1/12.98), (2) an interaction of the precession doublets at 19 and 23 kyr with the obliquity cycle ([1/19+1/23]-1/41 = 1/13.94), or (3) the third harmonic of obliquity (3/41 = 1/13.67). Unfortunately, none of these possibilities provides an exact match in period to the observed variance, nor are we aware of how these orbital interactions may be linked to specific physical mechanisms of climate change. While the discrepancies between the theoretical and observed frequencies could arise from age model errors, the lack of a plausible physical mechanism suggests the need for caution when interpreting these potential cycles. Additional work is needed to replicate this observation in other records and/or analysis with higher-order statistical methods such as bispectral analysis before definitive statements can be made regarding the nature of this longer-frequency suborbital variability.

The shorter cycles, from 11 to 5 kyr, require a higher-order response to orbital forcing (i.e., harmonics) or a nonlinear origin within the response of the climate system itself. Of potentially great significance is the identification of concentrations of variance at periods centered on 7.5-8.2 and 4.8-6.1 kyr. The variation in the estimated period of these two peaks is most likely due to uncertainties in the age model, which are untuned to variability at these frequencies. Could sub-Milankovitch peaks in the spectral ranges we observe arise as numerical artifacts resulting from the nonlinearity inherent in percent data? If we consider a simple system with two components (e.g., deep-sea carbonate and terrigenous input) that vary as independent linear responses y_1 and y_2 to orbital forcing x, (e.g. $y_1 = m_1x+b_1$; $y_2 = m_2x+b_2$) we see that expressing y_1 as a percentage of $(y_1 + y_2)$ results in a non-linear measure: $\%y_1 = 100(m_1x+b_1)/(m_1x+b_1 + m_2x+b_2)$. Despite this we do not believe that this is the underlying cause of the spectral peaks we observe because the spurious peaks arising in this way should not be band-limited to discrete frequency ranges. In addition, sub-Milankovitch variability has been observed by other studies using grayscale and reflectance data [*Bond et al.*, 1993;

Hagelberg et al., 1994; *Boyle*, 1997], magnetic susceptibility [*Moros et al.*, 1997], and isotope data [*Yiou et al.*, 1994; *Raymo et al.*, 1998]. This implies that its origin cannot be accounted for as a simple artifact of percentage data.

3.4. Heinrich-Like Cyclicity and Precessional Clipping

We believe the 7.5-8.2 kyr peak may be related to Heinrich-like variability, which exhibits a similar quasi-periodicity [e.g., *McIntyre and Molfino*, 1996]. The presence of a 7.5-8.2 kyr peak throughout the proxy percent carbonate record at Feni Drift provides several potentially important insights into the operation of the climate system. First, the Heinrich-like periodicity observed here cannot arise solely from ice sheet-bedrock dynamics as hypothesized by the "binge-purge" model of *MacAyeal* [1993a,b] and *Alley and MacAyeal* [1994]. If that were the case, one should not observe 7.5-8.2 kyr variability in the record before 2.5 or 2.75 Ma, prior to the intensification of Northern Hemisphere glaciation. Second, the presence of 7.5-8.2 kyr variability in the percent carbonate record prior to 2.75 Ma suggests that dilution of the percent carbonate signal by ice-rafted debris cannot be the sole cause of the observed variability in the proxy percent carbonate records. Alternative mechanisms for the cause of this variability could be shifts in carbonate production associated with changes in the location of the polar frontal zone or variations in carbonate dissolution associated with changes in the mixing ratio of northern component (NADW-like) and southern component (Antarctic Bottom Water (AABW) -like) waters at Feni Drift. Given the data at hand, we cannot distinguish between these two possibilities.

The spectral peak at 4.8-6.1 kyr is intriguing because it provides further insight into potential mechanisms of millennial-scale climate. *Hagelberg et al.*, [1994] report the presence of spectral peaks at 5 and 10-11 kyr in a 400 kyr rectified version of the precession record of *Berger and Loutre* [1988]. The reader should note that further details of the orbital solution described by *Berger and Loutre* [1988] were published by *Berger and Loutre* [1991], the more familiar source for this orbital solution. One potential physical link between the rectified precession record and climate is a mechanism referred to as equatorial "clipping" [e.g., *Short et al.*, 1991]. It has been postulated that the climate system should be very sensitive to precessional maxima (minima) at low latitudes because the out of phase response of the Northern and Southern Hemispheres to orbital variations means that low-latitude equatorial regions are influenced twice for each precessional maxima (minima). This phenomenon should result in increases to equatorial seasonality and intensification of monsoonal forcing. While *Hagelberg et al.* [1994] point out that these harmonics are not directly present in the astronomical forcing, they also note that the presence of such harmonics in climate records could result from either (1) a nonlinear response of the climate system to external forcing or (2) a nonlinearity in the climate recording mechanism. In the first case the climate system responds nonlinearly to an external forcing which is then linearly recorded by some climate proxy. Amplification of monsoonal variability in response to precessional rectification provides one such example [e.g., *Short et al.*, 1991; *Park et al.*, 1993; *Hagelberg et al.*, 1994]. In the second scenario, the climate system may respond linearly to external forcing, but the proxy recording system may be nonlinear in the way it "remembers" the climatic response. This scenario may be applicable to lake level records [*Crowley et al.*, 1992].

To asses whether a nonlinear process such as equatorial clipping ("rectification") could give rise to spectral peaks near 7.5-8.2 and 4.8-6.1 kyr, we performed an experiment similar to that of *Hagelberg et al.*, [1994] using a 5 Myr long precession record derived from the La93(1,1) solution. Similar results were also obtained using the *Berger and Loutre* [1991] orbital solution (not shown). The precession record was subdivided into nonoverlapping 1 Myr segments and windowed with a 1 Myr Hanning window prior to estimating power spectra for the full amplitude precession record and for clipped records with rectification thresholds of 0.1, 0.2, and 0.3 precession units (Figure 10a). This test differs from that of *Hagelberg et al.* [1994], who clipped only at zero amplitude precession and used a shorter 400 kyr precession record derived from the solution of *Berger and Loutre* [1988]. We formulated this test to simulate a climatic response with a gain sensitive to the magnitude of the external precessional forcing. The results indicate a translation of variance from the 19-23 kyr doublets (Figure 10b) to both longer- and shorter-frequency responses at 434, 122, 11.6 - 9.6, 8.6 - 6.7, and 5.8 - 5.2 kyr (Figure 10c). The higher frequency bands may represent the second, third and fourth harmonics of the primary precession doublets at 23 and 19 kyr. Variance transfers of this type were postulated by *Short et al.* [1991] and independently observed by *Pokras and Mix* [1987], *Park et al.* [1993], *Hagelberg et al.* [1994], and *Clemens and Tiedemann* [1997] for various components of the climate system. The presence of peaks at 6.7-8.6 and 5.2-5.8 kyr in the clipped precession record suggests that at least some of the variance observed in these frequency bands in the Feni Drift proxy percent carbonate record may arise from a nonlinear response to precessional forcing. *Hagelberg et al.* [1994] estimated as much as 30% of the variance in the 10-12 kyr band may be externally forced. Indeed, the presence of sub-Milankovitch peaks throughout the Feni Drift record suggest a "pacing" that may arise from orbital forcing. These results suggest the need for more climate-modeling studies designed to test the sensitivity the climate system to external forcing at sub-Milankovitch frequencies.

4. Conclusions

The relative brightness of diffuse reflectance measurements from ODP sites 980-984 are controlled largely by variation in sediment $CaCO_3$ content. Accordingly, a highly significant transfer function that accounts for 94% of the carbonate variance with an RMSE of 8.0% can be devised from the reflectance data. This relationship allows us to generate continuous records of proxy percent carbonate for the past 4.5 Myr at these sites. Strong correlations between proxy percent carbonate records from Ceara Rise in the equatorial Atlantic and Feni Drift in the North Atlantic allow us to transfer the orbitally tuned age model from Ceara Rise to Feni Drift. Power spectra of the Feni Drift proxy percent carbonate time series for time intervals ranging from 4.5-2.8, 2.4-0.95, and 0.95-0 Myr document the evolution of variance in the Milankovitch eccentricity, obliquity, and precession bands. Significant sub-Milankovitch climate variability is observed with periods centered near 7.6-8.4, and 4.8-6.1 kyr. The climate cycle of 7.6-8.4 kyr duration is present throughout the record and may be related to Heinrich-like periodicity. The presence of 7.6-8.4 kyr cyclicity in the percent carbonate record prior to the intensification of Northern Hemisphere glaciation suggests this Heinrich-like cyclicity must arise from some portion of the climate system other

than the dynamics of large ice sheets. The presence of variance peaks at 8.6 - 6.7 and 5.8 - 5.2 kyr in the clipped precession record suggests that at least some of the variance observed in these frequency bands in the Feni Drift proxy percent carbonate record may arise from a nonlinear response to precessional forcing driven by equatorial clipping.

Acknowledgments. We thank the captain and crew of the R/V JOIDES Resolution, the Leg 162 co-chief scientists, M. Raymo and E. Jansen. for their assistance at sea and the Leg 162 sedimentologists who helped operate the SCAT. W. Rugh provided assistance setting up the SCAT system on the R/V JOIDES Resolution. Samples for shipboard analysis were provided by the Ocean Drilling Program. D. Hodell and K. Venz kindly provided unpublished carbonate data. M. Lyle and P. Delaney provided helpful critical and editorial suggestions. This research was supported in part by a postcruise JOI/USSSP grant to JDO. This is LDEO scientific contribution 5884.

References

Alley. R.B.. and D.R. MacAyeal. Ice-rafted debris associated with binge/purge oscillations of the Laurentide ice sheet. *Paleoceanography. 9.* 503-511. 1994.

Balsam. W.L.. and B.C. Deaton. Sediment dispersal in the Atlantic Ocean: Evaluation by visible light spectra. *Rev. Aquat. Sci.. 4.* 411-447. 1991.

Balsam. W.L.. J.E. Damuth. and R.R. Schneider. Comparison of shipboard vs. shore-based spectral data from Amazon fan cores: Implications for interpreting sediment composition. *Proc. Ocean Drill. Program, Sci. Results. 155.* 1-23. 1997.

Berger. A.. and M.F. Loutre. New insolation values for the climate of the last 10 million years. *Sci. Rep. 1988/13,* Inst. d'Astron. et de Geophys. G. Lemaitre. Univ. Cath. de Louvain. Louvain-la-Neuve. Belgium. 1988.

Berger A.. and M.F. Loutre. Insolation values for the climate of the last 10 million of years. *Quat. Sci. Rev.. 10.* 297-317. 1991.

Bickert. T.. W.B. Curry. and G. Wefer. Late Pliocene to Holocene (2.6 to 0 Ma) western equatorial Atlantic deep water circulation: Inferences from benthic stable isotopes. ODP Leg 154. *Proc. Ocean Drill. Program, Sci. Results. 154.* 239-254. 1997.

Bond. G.. and R. Lotti. Iceberg discharges into the North Atlantic on millennial time scales during the last glaciation. *Science. 267.* 1005-1010. 1995.

Bond. G.. W.. Broecker. S. Johnsen. J. McManus. L. Labyerie. J. Jouzel. and G. Bonani. Correlations between climate records from North Atlantic sediments and Greenland ice. *Nature, 365.* 143-147. 1993.

Boyle. E.A.. Characteristics of the deep ocean carbon system during the past 150.000 years: ΣCO_2 distributions. deep water flow patterns. and abrupt climate change. *Proc. Natl. Acad. Sci, 94.* 8300-8307. 1997.

Channell. J.E.T.. D.A.Hodell. B. Lehman. Relative geomagnetic paleointensity and $\delta^{18}O$ at ODP Site 983 (Gardar Drift. North Atlantic) since 350 ka. *Earth Planet. Sci. Lett.. 153.* 103-118. 1997.

Clarke. F.J.J. and J.A. Compton. Correction methods for integrating-sphere measurement of hemispherical reflectance. *Color Res. and Appl., 11.* 253-262. 1986.

Clemens. S.. and R. Tiedemann. Eccentricity forcing of Pliocene-early Pleistocene climate revealed in a marine oxygen-isotope record. *Nature. 385.* 801-804. 1997.

Crowley T.J.. K.-Y. Kim. J.G. Mengel. and D.A. Short. Modeling 100.000-year climate fluctuations in pre-Pleistocene time series. *Science, 255.* 705-707. 1992.

Dansgaard W.. J.W.C. White. and S.J. Johnsen. The abrupt termination of the Younger Dryas climate event. *Nature, 339,* 532-534. 1989.

Deaton. B.C.. and W.L. Balsam. Visible spectroscopy: A rapid method for determining hematite and goethite concentrations in geological material. *J. Sediment. Petrol., 61.* 628-632. 1991.

Ghil. M.. and H. LeTreut. A climate model with cryodynamics and geodynamics. *J. Geophys. Res. 86.* 5262-5270. 1981.

Hagelberg. T.K.. G. Bond. and P. deMenocal. Milankovitch band forcing of sub-Milankovitch climate variability during the Pleistocene. *Paleoceanography, 9.* 545-558. 1994.

Harris. S.E.. A.C. Mix. and T. King. Biogenic and terrigenous sedimentation at Ceara Rise. western tropical Atlantic. supports pliocene-pleistocene deep-water linkage between hemispheres. *Proc. Ocean Drill. Program, Sci. Results, 154.* 331-348. 1997.

Haug. G.H.. M.A. Maslin. M. Sarnthein. R. Stax. and R. Tiedemann. Evolution of northwest Pacific sedimentation patterns since 6 Ma (Site 882). *Proc. Ocean Drill. Program, Sci. Results, 145.* 293-314. 1995.

Hays. J.D.. J. Imbrie. N.J. Shackleton. Variations in the Earth's orbit: Pacemaker of the ice ages. *Science. 194* 1121-1132. 1976.

Hughen. K.. J.T. Overpeck. L.C. Peterson. and S. Trumbore. Rapid climate changes in the tropical Atlantic region during the last deglaciation. *Nature. 380.* 51-54. 1996.

Imbrie. J.. et al.. The orbital theory of Pleistocene climate: Support from a revised chronology of the marine $\delta^{18}O$ record. in *Milankovitch and Climate.* vol. 1. edited by A. Berger et al.. pp. 269-305. D. Reidel. Norwell. Mass. 1984.

Imbrie. J.. et al.. On the structure and origin of the major glaciation cycles. 1. Linear responses to Milankovitch forcing. *Paleoceanography, 7,* 701-738. 1992.

Imbrie. J.. et al.. On the structure and origin of the major glaciation cycles. 2. The 100.000-year cycle. *Paleoceanography, 8,* 699-735. 1993.

Jansen E.. and J. Sjoholm. Reconstruction of glaciation over the past 6 Myr from ice-borne deposits in the Norwegian Sea. *Nature. 349.* 600-603. 1991.

Koc-Karpuz. N.. and E. Jansen. A high-resolution diatom record of the last deglaciation from the SE Norwegian Sea: Documentation of rapid climatic changes. *Paleoceanography, 7,* 499-520. 1992

Lasker. J.. The chaotic motion of the solar system: A numerical estimate of the size of the chaotic zone. *Icarus. 88.* 266-291. 1990.

Lasker. J.. J. Jousel. and F. Boudin. Orbital, precessional. and insolation quantities for the Earth from -20 Myr to +10 Myr. *Astron. and Astrophys.. 270.* 522-533. 1993.

Leg 154 Shipboard Scientific Party. Explanatory notes. *Proc. Ocean Drill. Program, Initial Rep.. 154.* 14: Appendix A. 1995.

Leg 162 Shipboard Scientific Party. Sites 980/981. *Proc. Ocean Drill. Program, Initial Rep.. 162.* 49-90. 1996a.

Leg 162 Shipboard Scientific Party, Sites 982. *Proc. Ocean Drill. Program, Initial Rep., 162.* 91-138. 1996b.

Leg 162 Shipboard Scientific Party. Sites 983. *Proc. Ocean Drill. Program, Initial Rep.. 162.* 139-168. 1996c.

Leg 162 Shipboard Scientific Party. Site 984. *Proc. Ocean Drill. Program, Initial Rep.. 162,* 169-222. 1996d.

Lehman. S.. and L.D. Keigwin. Sudden changes in North Atlantic circulation during the last deglaciation. *Nature. 356.* 757-762. 1992.

MacAyeal. D.R.. A low-order model of the Heinrich event cycle. *Paleoceanography. 8,* 767-773. 1993a.

MacAyeal. D.R.. Binge/purge oscillations of the Laurentide Ice Sheet as a cause of the North Atlantic's Heinrich events. *Paleoceanography. 8.* 775-784. 1993b.

Mann M.E.. and J.M. Lees. Robust estimation of background noise and signal detection in climatic time series *Clim. Change. 33.* 409-445. 1996.

Martinson. D.G.. N.G. Pisias. J.D. Hays. J. Imbrie. T. Moore Jr. and N. J. Shackleton. Age dating and the orbital theory of the ice ages: development of a high-resolution 0 to 300.000-year chronostratigraphy. *Quat. Res. 27.* 1-29. 1987.

Maslin. M.A.. G.H. Haug. M. Sarnthein. R. Tiedemann. H. Erlenkeuser. and R. Stax. Northwest Pacific Site 882: the initiation of Northern Hemisphere glaciation. *Proc. Ocean Drill. Program, Sci. Results, 145.* 315-329. 1995.

McIntyre. A. and B. Molfino. Forcing of Atlantic equatorial and subpolar millennial cycles by precession. *Science. 274.* 1867-1870. 1996.

Mix. A.C.. W. Rugh. N.G. Pisias. and S. Veirs. Leg 138 Shipboard sedimentologists. and the leg 138 Scientific Party. Color reflectance spectroscopy: a tool for rapid characterization of deep-

sea sediments, *Proc. Ocean Drill. Program, Init. Rep., 138*, 67-77, 1992.

Mix, A.C, S.E. Harris, and T.R. Janecek, Estimating lithology from nonintrusive reflectance spectra: Leg 138, *Proc. Ocean Drill. Program, Sci. Rep., 138*, 413-427, 1995.

Molfino, B., and A. McIntyre, Precessional forcing of nutricline dynamics in the equatorial Atlantic, *Science, 249*, 766-769, 1990.

Moros, M., R. Endler, K.S. Lackschewitz, H.-J. Wallrabe-Adams, J. Mienert and W. Lemke, Physical properties of Reykjanes Ridge sediments and their linkage to high-resolution Greenland Ice Sheet Project 2 ice core data, *Paleoceanography, 12*, 687-695, 1997.

Ortiz, J., et al., Data report: Spectral reflectance observations from Leg 162 sediments, *Proc. Ocean Drill. Program, Sci. Results*, in press, 1999.

Overpeck, J., L.C. Peterson, N. Kipp, J. Imbrie, and D. Rind, Climate change in the circum-North Atlantic region during the last deglaciation, *Nature, 338*, 553-557, 1989.

Park, J., S. d'Hondt, J. King, and C. Gibson, Late Cretaceous precessional cycles in double time: A warm-Earth Milankovitch response, *Science, 261*, 1431-1434, 1993.

Pokras, E.M., and A.C. Mix, Earth's precessional cycle and quaternary climate change in tropical Africa, *Nature, 326*, 486-487, 1987.

Press, W.H., S.A. Teukolsky, W.T. Vetterling, and B.P. Flannery, *Numerical Recipes in Fortran: The art of Scientific Computing* (2nd ed.), pp. 180-184, Cambridge Press, New York, 1992.

Raymo, M.E., W.F. Ruddiman, J. Backman, B.M. Clement, and D.G. Martinson, Late Pliocene variations in Northern Hemisphere ice sheets and North Atlantic deep water circulation, *Paleoceanography, 4*, 413-446, 1989.

Raymo, M.E., K. Ganley, S. Carter, D.W. Oppo, and J. McManus, Millennial-scale climate instability during the early Pleistocene epoch, *Nature, 392*, 699-702, 1998.

Rind D., D. Peteet, W.S. Broecker, A. Mcintyre, and W. Ruddiman, The impact of cold North Atlantic sea surface temperatures on climate: Implications for the Younger Dryas cooling (11-10 k), *Clim. Dyn., 1*, 3-33, 1986.

Ruddiman, W.F., and A. McIntyre, An evaluation of ocean-climate theories in the North Atlantic, in *Milankovitch and Climate*, vol. 1, edited by A. Berger et al., pp. 671-686, D. Reidel, Norwell, Mass., 1984.

Ruddiman, W.F., and M.E. Raymo, Northern hemisphere climate regimes during the past 3 Ma: Possible tectonic connections, *Philos. Trans. R. Soc. London Ser. B, 318*, 411-430, 1988.

Short, D.A., J.G. Mengel, T.J. Crowley, W.T. Hyde, and G.R. North, Filtering of Milankovitch cycles by Earth's geography, *Quat. Res., 35*, 157-173, 1991.

Thompson, D.J., Spectrum estimation and harmonic analysis, *Proc. IEEE, 70*, 1055-1096, 1982.

Tiedemann, R., and S.O. Franz, Deep-water circulation, chemistry, and terrigenous sediment supply in the equatorial atlantic during the pliocene, 3.3-2.6 Ma and 5-4.5 Ma, *Proc. Ocean Drill. Program, Sci. Res., 154*, 299-318, 1997.

Venz, K., D.A. Hodell, C. Stanton, and D.A. Warnke, A 1 Myr record of glacial North Atlantic intermediate water variability from ODP site 982 in the northeast Atlantic, *Paleoceanography, in press*, 1999.

Yiou, P., M. Ghil, J. Jouzel, D. Paillard, and R. Vautard, Nonlinear variability of the climatic system from singular and power spectra of late Quaternary records, *Clim. Dyn., 9*, 371-389, 1994.

S. Harris, Sea Education Association (SEA) P.O. Box 6, Woods Hole MA 02543.

A. Mix, College of Oceanic and Atmospheric Sciences, Oregon State University, Corvallis, OR 97330-5503.

S. O'Connell, Department of Earth and Environmental Sciences, 265 Church Street, Wesleyan University, Middletown, CT 06459.

J. Ortiz, Lamont-Doherty Earth Observatory of Columbia University, R.T. 9W, Palisades, NY 10964. (jortiz@columbia.edu)

(Received February 23, 1998;
revised November 17, 1998;
accepted November 19, 1998.)